

Supporting Information

Se-doped $\text{Li}_6\text{PS}_5\text{Cl}$ and $\text{Li}_{5.5}\text{PS}_{4.5}\text{Cl}_{1.5}$ with improved ionic conductivity and interfacial compatibility: a high-throughput DFT study

Ming Jiang¹, Zhi-Wen Chen², Adwitiya Rao², Li-Xin Chen², Xiao-Tao Zu^{3,*}, Chandra Veer Singh^{2,4,*}

¹Institute of Physical Science and Information Technology, Anhui University, Hefei 230601, China

²Department of Materials Science and Engineering, University of Toronto, Ontario M5S 3E4, Canada

³Yangtze Delta Region Institute (Huzhou), University of Electronic Science and Technology of China, Huzhou 313001, China

⁴Department of Mechanical and Industrial Engineering, University of Toronto, Ontario M5S 3G8, Canada

Table S1. Atomic occupancy in $\text{Li}_6\text{PS}_5\text{Cl}$ and $\text{Li}_{5.5}\text{PS}_{4.5}\text{Cl}_{1.5}$.

Atom	Wyckoff Position	Occupancy ($\text{Li}_6\text{PS}_5\text{Cl}$)	Occupancy ($\text{Li}_{5.5}\text{PS}_{4.5}\text{Cl}_{1.5}$)
Li_1	$48h$	0.456	0.440
P_1	$4b$	1.000	1.000
Cl_1	$4a$	0.615	0.370
S_1	$4a$	0.385	0.630
Cl_2	$4d$	0.834	0.630
S_2	$4d$	0.166	0.370
S_3	$16e$	0.618	1.000

Table S2. Total energy and lattice parameter of Li₆PS₅Cl obtained from DFT calculations. The most stable structure is indicated in bold.

Structure ID.	Total energy (eV)	Lattice constant (Å)			Degree (°)		
		a	b	c	α	β	γ
1	-215.62	9.91	10.08	10.02	89.92	88.12	89.82
2	-216.05	10.03	9.91	9.89	90.19	89.78	90.45
3	-216.27	9.88	9.95	9.98	89.97	91.54	90.63
4	-216.42	9.97	9.92	9.98	89.89	89.18	90.48
5	-216.25	10.06	9.89	9.99	89.04	89.58	90.36
6	-216.18	10.04	9.97	9.94	89.25	88.69	87.14
7	-216.87	9.98	9.96	9.92	90.77	89.53	90.68
8	-216.41	9.92	9.89	9.91	88.94	88.74	89.30
9	-216.03	9.93	9.94	10.09	89.05	88.64	88.02
10	-216.21	9.97	10.05	9.85	89.22	88.99	89.37

Table S3. Total energy and lattice parameter of $\text{Li}_{5.5}\text{PS}_{4.5}\text{Cl}_{1.5}$ obtained from DFT calculations. The most stable structure is indicated in bold.

Structure ID.	Total energy (eV)	Lattice constant (Å)			Degree (°)		
		a	b	c	α	β	γ
1	-203.63	10.18	9.92	9.86	89.46	92.02	89.32
2	-203.45	9.87	10.08	10.21	91.53	89.82	90.64
3	-203.72	9.82	10.03	10.03	90.24	88.88	89.74
4	-203.71	10.17	9.79	9.88	89.52	91.99	88.35
5	-203.39	9.99	9.74	10.08	87.64	90.86	90.07
6	-203.34	9.79	10.06	9.88	89.26	89.14	88.83
7	-203.49	9.85	10.02	9.99	89.04	90.19	89.50
8	-202.17	9.88	9.91	9.93	89.55	91.92	91.97
9	-203.15	10.17	9.81	9.86	89.15	90.05	89.07
10	-202.34	9.91	9.92	9.86	90.04	89.20	88.89

Table S4. Total energy of $\text{Li}_6\text{PS}_{5-x}\text{Se}_x\text{Cl}$ ($x = 1 \sim 4$) obtained from DFT calculations.

The most stable structure for each Se-doped $\text{Li}_6\text{PS}_5\text{Cl}$ is indicated in bold.

Structure ID.	Total energy (eV)			
	$\text{Li}_6\text{PS}_4\text{SeCl}$	$\text{Li}_6\text{PS}_3\text{Se}_2\text{Cl}$	$\text{Li}_6\text{PS}_2\text{Se}_3\text{Cl}$	$\text{Li}_6\text{PS}_4\text{SeCl}$
1	-212.56	-208.15	-204.96	-201.27
2	-212.94	-208.99	-204.98	-201.15
3	-212.73	-208.66	-204.91	-201.09
4	212.76	-208.53	-204.95	-200.89
5	-212.83	-208.96	-205.05	-201.09
6	-212.28	-208.59	-204.82	-201.29
7	-212.87	-208.90	-204.88	-201.08
8	-212.82	-208.84	-204.91	-201.12
9	-213.09	-209.05	-205.27	-201.09
10	-212.80	-208.88	-204.92	-201.22

Table S5. Total energy of $\text{Li}_{5.5}\text{PS}_{4.5-x}\text{Se}_x\text{Cl}_{1.5}$ ($x=1 \sim 3$) obtained from DFT calculations.

The most stable structure for each Se-doped $\text{Li}_{5.5}\text{PS}_{4.5}\text{Cl}_{1.5}$ is indicated in bold.

Structure ID.	Total energy (eV)		
	$\text{Li}_6\text{PS}_{3.5}\text{SeCl}$	$\text{Li}_6\text{PS}_{2.5}\text{Se}_2\text{Cl}$	$\text{Li}_6\text{PS}_{1.5}\text{Se}_3\text{Cl}$
1	-199.77	-195.97	-192.61
2	-200.18	-196.63	-192.61
3	-200.26	-196.33	-192.55
4	-200.01	-196.28	-192.36
5	-199.92	-196.12	-192.11
6	-200.02	-196.42	-192.51
7	-199.75	-196.33	-192.17
8	-199.74	-196.12	-192.36
9	-199.76	-196.22	-192.66
10	-199.73	-195.81	-191.88

Table S6. Lattice parameter of the most stable $\text{Li}_6\text{PS}_{5-x}\text{Se}_x\text{Cl}$ ($x = 1 \sim 4$) structures.

	$\text{Li}_6\text{PS}_4\text{SeCl}$	$\text{Li}_6\text{PS}_3\text{Se}_2\text{Cl}$	$\text{Li}_6\text{PS}_2\text{Se}_3\text{Cl}$	$\text{Li}_6\text{PSSe}_4\text{Cl}$
a (Å)	10.20	10.32	10.67	10.68
b (Å)	10.22	10.66	10.05	10.25
c (Å)	10.27	10.11	10.70	10.92
α (°)	90.14	90.21	92.13	90.30
β (°)	88.18	86.90	90.00	90.30
γ (°)	92.09	90.57	90.00	92.64
V (Å ³)	1069.09	1110.71	1146.05	1193.13

Table S7. The lattice parameter of the most stable $\text{Li}_{5.5}\text{PS}_{4.5-x}\text{Se}_x\text{Cl}_{1.5}$ ($x = 1 \sim 3$) structure.

	$\text{Li}_{5.5}\text{PS}_{3.5}\text{SeCl}_{1.5}$	$\text{Li}_{5.5}\text{PS}_{2.5}\text{Se}_2\text{Cl}_{1.5}$	$\text{Li}_{5.5}\text{PS}_{1.5}\text{Se}_3\text{Cl}_{1.5}$
a (Å)	9.90	9.97	10.11
b (Å)	10.14	10.27	10.34
c (Å)	10.08	10.22	10.39
α (°)	89.95	90.01	89.79
β (°)	89.66	89.62	89.67
γ (°)	90.22	90.24	89.41
V (Å ³)	1012.06	1045.94	1085.29

Table S8. Phase equilibria and reaction energy (ΔE_D) of $\text{Li}_6\text{PS}_{5-x}\text{Se}_x\text{Cl}$ ($x = 0 \sim 4$) at the interface with LiCoO_2 and $\text{Li}_{0.5}\text{CoO}_2$.

C_{SSE}	$C_{\text{electrode}}$	x_m	Phase equilibria at x_m	ΔE_D (meV/atom)
$\text{Li}_6\text{PS}_5\text{Cl}$	LiCoO_2	0.53	LiCl , Li_3PO_4 , Co_9S_8 , Li_2SO_4 , Li_2S	-302.12
	$\text{Li}_{0.5}\text{CoO}_2$	0.51	Li_2SO_4 , Co_9S_8 , Li_3PO_4 , LiCl , Li_2S	-434.98
$\text{Li}_6\text{PS}_4\text{SeCl}$	LiCoO_2	0.57	Li_2S , Co_9S_8 , LiCl , Li_2SO_4 , CoSe_2 , Li_3PO_4	-302.24
	$\text{Li}_{0.5}\text{CoO}_2$	0.51	Co_9S_8 , Li_3PO_4 , LiCl , Li_2SO_4 , Li_2S , Li_2Se	-434.98
$\text{Li}_6\text{PS}_3\text{Se}_2\text{Cl}$	LiCoO_2	0.61	Co_9S_8 , Li_2S , Li_3PO_4 , CoSe_2 , LiCl , Li_2SO_4	-310.77
	$\text{Li}_{0.5}\text{CoO}_2$	0.53	Li_2SO_4 , Li_3PO_4 , Co_9S_8 , LiCl , Co_3Se_4 , Li_2Se	-434.87
$\text{Li}_6\text{PS}_2\text{Se}_3\text{Cl}$	LiCoO_2	0.62	Li_2S , Co_9S_8 , Li_2Se , Li_3PO_4 , CoSe_2 , LiCl	-319.45
	$\text{Li}_{0.5}\text{CoO}_2$	0.55	LiCl , Co_9S_8 , Co_3Se_4 , Li_2Se , Li_2SO_4 , Li_3PO_4	-433.68
$\text{Li}_6\text{PSSe}_4\text{Cl}$	LiCoO_2	0.62	CoSe_2 , Li_2S , LiCl , Li_2Se , Co_9S_8 , Li_3PO_4	-328.28
	$\text{Li}_{0.5}\text{CoO}_2$	0.51	Li_2SO_4 , Li_3PO_4 , Co_9S_8 , Co_9Se_8 , LiCl , Li_2Se	-432.70

Table S9. Phase equilibria and reaction energy (ΔE_D) of $\text{Li}_{5.5}\text{PS}_{4.5-x}\text{Se}_x\text{Cl}_{1.5}$ ($x = 0 \sim 3$) at the interface with LiCoO_2 and $\text{Li}_{0.5}\text{CoO}_2$.

C_{SSE}	$C_{\text{electrode}}$	x_m	Phase equilibria at x_m	ΔE_D (meV/atom)
$\text{Li}_{5.5}\text{PS}_{4.5}\text{Cl}_{1.5}$	LiCoO_2	0.52	LiCl , Li_2S , Li_2SO_4 , Co_9S_8 , Li_3PO_4	-308.41
	$\text{Li}_{0.5}\text{CoO}_2$	0.50	Li_3PO_4 , Co_9S_8 , Li_2S , LiCl , Li_2SO_4	-443.75
$\text{Li}_{5.5}\text{PS}_{3.5}\text{SeCl}_{1.5}$	LiCoO_2	0.56	CoSe_2 , Co_9S_8 , Li_2SO_4 , Li_2S , LiCl , Li_3PO_4	-312.97
	$\text{Li}_{0.5}\text{CoO}_2$	0.52	CoSe_2 , Li_3PO_4 , Li_2Se , Li_2SO_4 , Co_9S_8 , LiCl	-444.35
$\text{Li}_{5.5}\text{PS}_{2.5}\text{Se}_2\text{Cl}_{1.5}$	LiCoO_2	0.60	CoSe_2 , LiCl , Li_2SO_4 , Co_9S_8 , Li_2S , Li_3PO_4	-322.69
	$\text{Li}_{0.5}\text{CoO}_2$	0.55	LiCl , Li_3PO_4 , CoSe_2 , Li_2SO_4 , Li_2Se , Co_9S_8	-443.70
$\text{Li}_{5.5}\text{PS}_{1.5}\text{Se}_3\text{Cl}_{1.5}$	LiCoO_2	0.61	CoSe_2 , Li_3PO_4 , Li_2Se , Li_2S , LiCl , Co_9S_8	-332.08
	$\text{Li}_{0.5}\text{CoO}_2$	0.59	Co_9S_8 , LiCl , CoSe_2 , Li_2SO_4 , Li_2Se	-443.10

Table S10. Phase equilibria and reaction energy (ΔE_D) of $\text{Li}_6\text{PS}_{5-x}\text{Se}_x\text{Cl}$ ($x = 0 \sim 4$) at the interface with LiFePO_4 and FePO_4 .

C_{SSE}	$C_{\text{electrode}}$	x_m	Phase equilibria at x_m	ΔE_D (meV/atom)
$\text{Li}_6\text{PS}_5\text{Cl}$	LiFePO_4	0.39	Li_3PO_4 , FePS, $\text{Li}_4\text{P}_2\text{O}_7$, LiCl, FeS_2	-99.75
	FePO_4	0.45	LiCl, FeS_2 , $\text{Li}_4\text{P}_2\text{O}_7$, FePS, LiPO_3	-196.86
$\text{Li}_6\text{PS}_4\text{SeCl}$	LiFePO_4	0.43	FePS, Se, FeSe_2 , Li_3PO_4 , FeS_2 , LiCl	-101.73
	FePO_4	0.45	FeSe_2 , LiCl, LiPO_3 , FeS_2 , FePS, $\text{Li}_4\text{P}_2\text{O}_7$	-196.53
$\text{Li}_6\text{PS}_3\text{Se}_2\text{Cl}$	LiFePO_4	0.43	FeS_2 , FePS, FeSe_2 , LiCl, Li_3PO_4 , Se	-107.28
	FePO_4	0.45	FeS_2 , FeSe_2 , $\text{Li}_4\text{P}_2\text{O}_7$, FePS, LiCl, LiPO_3	-202.34
$\text{Li}_6\text{PS}_2\text{Se}_3\text{Cl}$	LiFePO_4	0.43	LiCl, FeS_2 , FePS, FeSe_2 , Se, Li_3PO_4	-112.83
	FePO_4	0.50	FeS_2 , Se, FeSe_2 , LiCl, $\text{Li}_4\text{P}_2\text{O}_7$, FePS	-208.47
$\text{Li}_6\text{PSSe}_4\text{Cl}$	LiFePO_4	0.43	FeSe_2 , Li_3PO_4 , Se, LiCl, FePS	-118.59
	FePO_4	0.50	FePS, FeS_2 , LiCl, FeSe_2 , $\text{Li}_4\text{P}_2\text{O}_7$, Se	-215.19

Table S11. Phase equilibria and reaction energy (ΔE_D) of $\text{Li}_{5.5}\text{PS}_{4.5-x}\text{Se}_x\text{Cl}_{1.5}$ ($x = 0 \sim 3$) at the interface with LiFePO_4 and FePO_4 .

C_{SSE}	$C_{\text{electrode}}$	x_m	Phase equilibria at x_m	ΔE_D (meV/atom)
$\text{Li}_{5.5}\text{PS}_{4.5}\text{Cl}_{1.5}$	LiFePO_4	0.40	$\text{Li}_4\text{P}_2\text{O}_7$, Li_3PO_4 , FeS_2 , LiCl , FePS	-87.52
	FePO_4	0.46	LiPO_3 , LiCl , FePS , FeS_2 , $\text{Li}_4\text{P}_2\text{O}_7$	-177.68
$\text{Li}_{5.5}\text{PS}_{3.5}\text{SeCl}_{1.5}$	LiFePO_4	0.45	Se , FePS , LiCl , $\text{Li}_4\text{P}_2\text{O}_7$, FeS_2 , Li_3PO_4	-91.61
	FePO_4	0.46	FeSe_2 , FeS_2 , LiPO_3 , $\text{Li}_4\text{P}_2\text{O}_7$, FePS , LiCl	-180.63
$\text{Li}_{5.5}\text{PS}_{2.5}\text{Se}_2\text{Cl}_{1.5}$	LiFePO_4	0.47	FeS_2 , LiCl , FePS , FeSe_2 , Se , Li_3PO_4	-98.99
	FePO_4	0.46	FePS , $\text{Li}_4\text{P}_2\text{O}_7$, LiCl , LiPO_3 , FeSe_2 , FeS_2	-187.01
$\text{Li}_{5.5}\text{PS}_{1.5}\text{Se}_3\text{Cl}_{1.5}$	LiFePO_4	0.47	Li_3PO_4 , FePS , FeSe_2 , Se , LiCl , FeS_2	-105.62
	FePO_4	0.46	FeS_2 , FeSe_2 , FePS , $\text{Li}_4\text{P}_2\text{O}_7$, LiPO_3 , LiCl	-193.51

Figure S1. Crystal structure of (a) - (d) $\text{Li}_6\text{PS}_{5-x}\text{Se}_x\text{Cl}$ ($x = 1 \sim 4$) and (e) - (g) $\text{Li}_{5.5}\text{PS}_{4.5-x}\text{Se}_x\text{Cl}_{1.5}$ ($x = 1 \sim 3$). The blue, yellow, orange, watchet and purple spheres represent the Li, S, Cl, P and Se atoms, respectively.

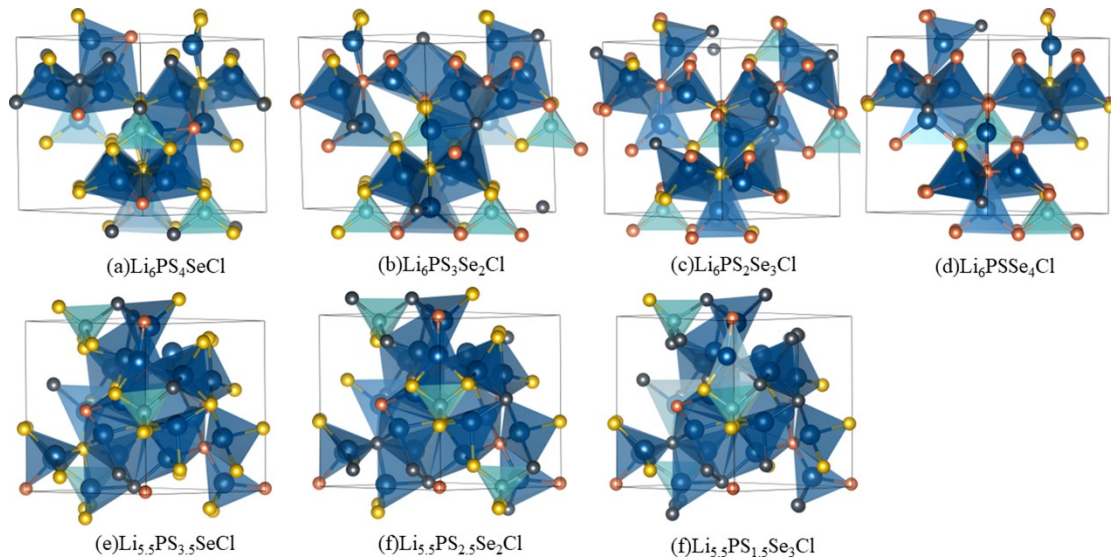


Figure S2. The mean square displacement (MSD) of Li^+ ions in (a) $\text{Li}_6\text{PS}_5\text{Cl}$, (b) $\text{Li}_6\text{PS}_4\text{SeCl}$, (c) $\text{Li}_6\text{PS}_3\text{Se}_2\text{Cl}$, (d) $\text{Li}_6\text{PS}_2\text{Se}_3\text{Cl}$ and (e) $\text{Li}_6\text{PSSe}_4\text{Cl}$ during 120 ps simulation time. (f) Diffusivity and activation energy of $\text{Li}_6\text{PS}_{5-x}\text{Se}_x\text{Cl}$ ($x = 0 \sim 4$) deduced from AIMD simulations at elevated temperatures ranging from 500 to 1000 K.

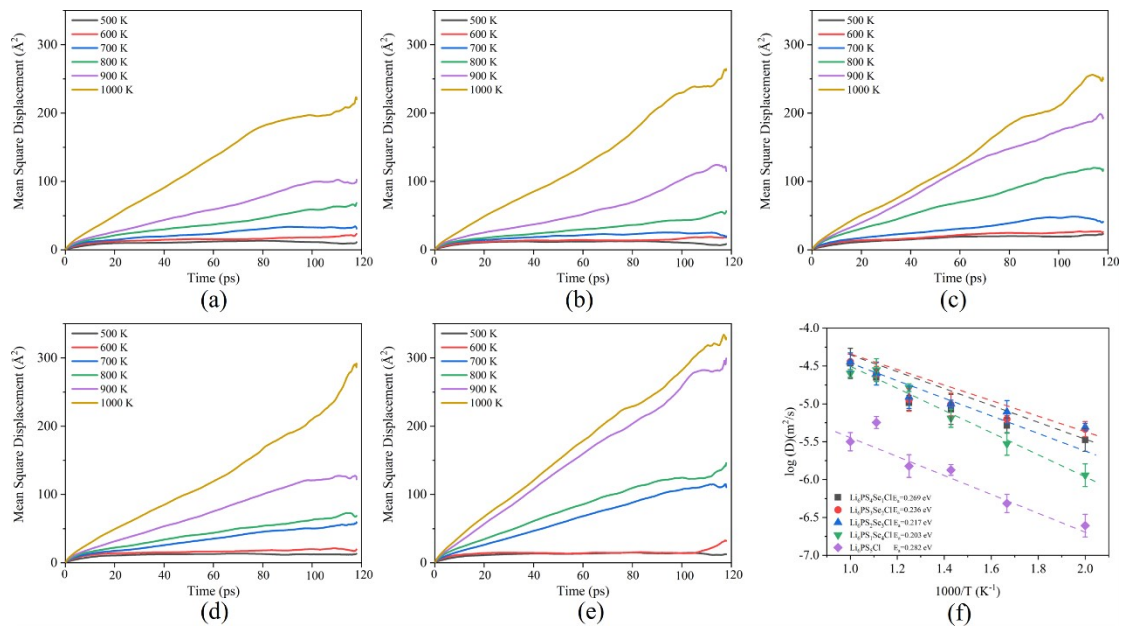


Figure S3. The mean square displacement (MSD) of Li^+ ions in (a) $\text{Li}_{5.5}\text{PS}_{4.5}\text{Cl}_{1.5}$, (b) $\text{Li}_{5.5}\text{PS}_{3.5}\text{SeCl}_{1.5}$, (c) $\text{Li}_{5.5}\text{PS}_{2.5}\text{Se}_2\text{Cl}_{1.5}$ and (d) $\text{Li}_{5.5}\text{PS}_{1.5}\text{Se}_3\text{Cl}_{1.5}$ during 120 ps simulation time. (e) Diffusivity and activation energy of $\text{Li}_{5.5}\text{PS}_{4.5-x}\text{Se}_x\text{Cl}_{1.5}$ ($x = 0 \sim 3$) deduced from AIMD simulations at elevated temperatures ranging from 500 to 1000 K.

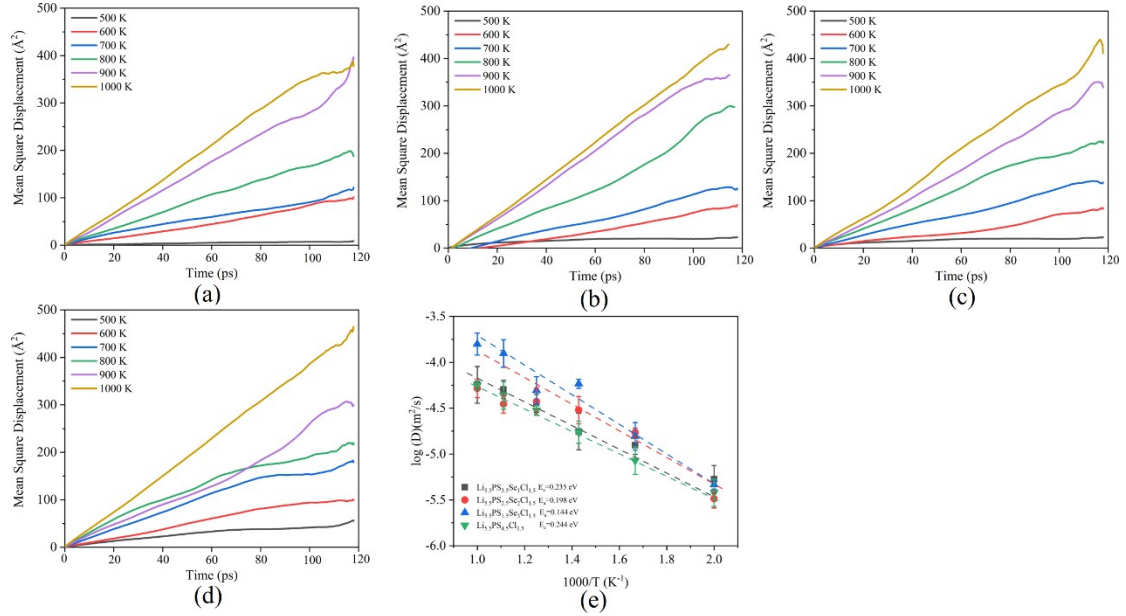


Figure S4. The Li^+ migration pathway of (a) $\text{Li}_6\text{PS}_5\text{Cl}$ and (b) $\text{Li}_{5.5}\text{PS}_{4.5}\text{Cl}_{1.5}$ at 500 K. The blue, green, yellow and red spheres represent the Li, P, S and Cl atoms, respectively. The blue line represents the Li^+ migration pathway during 120 ps simulation time.

